Potential-barrier model at metal surfaces: Application to analyses of low-energy electron-diffraction fine-structure experiments

E. E. Mola,* C. A. Paola, and J. L. Vicente
Instituto de Investigaciones Fisicoquímicas Teóricas y Aplicadas, Division Quimica Teórica, Sucursal 4, Casilla de Correo 16, La Plata 1900, Argentina
(Received 29 May 1991)

We propose a model for the potential barrier for electrons crossing a metal surface, in which (1) we reproduce the effective potential of Lang and Kohn, in fact, better than any approximation in the existing literature and (2) we approach the classical image potential for large separation from the surface. Our potential does not diverge as the electron approaches the surface and goes over smoothly to the electron-electron interaction potential in the bulk. It reproduces the first peak in the effective potential of Lang and Kohn, which is a Friedel oscillation. We achieve better agreement with the Lang-Kohn potential than Jennings, Jones, and Weinert in their barrier model. This makes our model useful in the analysis of low-energy electron-diffraction fine-structure experiments. Our simple barrier model allows analytical solutions of the Schrödinger equation in the density-functional formalism.

I. INTRODUCTION

There has been renewed interest in the electron-metal surface potential in the past few years. The detailed knowledge of this potential is of great importance for a correct interpretation of recent experimental observations of a class of surface states in metals[1,2] which originate from the imagelike tail of the surface potential. It is generally accepted that at large distances from the surface, the electron comes under the influence of the classical image potential

$$v_{\rm im}(z)=-\frac{1}{4(z-z_0)}\ , \tag{1}$$

where z is the distance of the electron to the surface, and z_0 the position of the image plane. This formula leads to a divergence when $z\rightarrow z_0$. Furthermore, the potential energy of the electron inside the crystal (the "inner potential") is approximately constant (for transition metals it is approximately equal to 12 eV) when the incident electron energy is below 50 eV. Like the work functions, the potential of the electron inside the metal depends on the crystal face.[3] An excellent review by Jones and Jennings[4] summarizes the present state of this problem. The difficulties with the image potential have initiated the development of simple model barriers to describe the electron-surface interaction.

(i) The simple step barrier:

$$V(z)=\begin{cases}0 & \text{if } z\geq z_0\\ -V_0 & \text{otherwise}\ ,\end{cases} \tag{2}$$

where V_0 is the inner potential and z_0 is the location of the image plane.

(ii) The exponential barrier:

$$V(z)=-V_0/\{1+\exp[B(z-z_0)]\}\ , \tag{3}$$

where B is an arbitrary constant and the other symbols have their usual meanings.

(iii) The truncated image barrier:

$$V(z)=\begin{cases}-1/4(z-z_0)\ , & z\geq z_c\\ -V_0\ , & z\leq z_c\ ,\end{cases} \tag{4}$$

which introduces an image form far from the surface and truncates it at z_c, where $V(z_c)=-V_0$, with V_0 the inner potential of the crystal.

(iv) The modified image surface potential-energy barrier: Read and Jennings[5] improved the previous barrier model by including a $(z-z_0)^{-2}$ term to provide a smooth transition to $-V_0$.

(v) Dietz, McRae, and Campbell[6] recognized the need for a barrier in which the potential-energy function $V(z)$ approaches the image form as $z\rightarrow\infty$, but which "saturates" and approaches the inner potential within the solid. Their model potential is

$$\mathrm{Re}V(z)=\begin{cases}-1/[4(z-z_0)]\ , & z>z_1\\ -V_1+z/[4(z-z_0)^2]\ , & z_1\geq z\geq z_c\\ -V_0\ , & z<z_0\ .\end{cases} \tag{5a}$$

Here V_0 is the inner potential, V_1 is the barrier height at the topmost layer of atoms ($z=0$), z_0 is the image plane location, z_1 is the point at which saturation begins, and z_c is the point at which the inner potential is reached. Inelastic scattering is represented by the imaginary part of the barrier potential,

$$\mathrm{Im}V(z)=\begin{cases}U_1\exp(-az^2)\ , & z\geq z_0\\ U_1 & \text{otherwise}\ .\end{cases} \tag{5b}$$

U_1 and a are adjusted to obtain the correct ratio of peak heights between the fine structure and the Bragg peaks. In this barrier model the step at z_c gives rise to spurious reflections,[7] which complicate the simulation of high-resolution low-energy electron-diffraction (LEED) spec-

tra. For this reason Jennings, Jones, and Weinert[3] (JJW) sought a more realistic saturated image barrier. Lang and Kohn[8] (LK) have calculated self-consistently the effective potential for an electron near the surface of jellium at various electron densities. Jennings, Jones, and Weinert found that the effective potential calculated by LK can be fitted well by a saturated image barrier of the form

$$V(z)=\begin{cases} -\dfrac{1}{4(z-z_0)}\{1-\exp[-\lambda(z-z_0)]\} & \text{if } z>z_0 \\ -\dfrac{V_0}{A\exp[B(z-z_0)]+1} & \text{otherwise .} \end{cases} \tag{6}$$

Here A and B are constants determined by matching $V(z)$ and its derivative at the reference plane $z=z_0$, so that $B=V_0/A$ and $A=-1+4V_0/\lambda$. Unfortunately, neither the JJW equation nor any barrier models proposed so far taken into consideration the well-defined effective potential minimum calculated by LK.[8] This minimum is an important characteristic of the effective potential especially at low electron densities. This minimum is placed inside the jellium and emerges as a consequence of electron-density Friedel oscillations near the jellium edge. Such oscillations are found in the effective potential of thin metal films by Mola and Vicente,[9] where for a lower electron density, one gets a deeper effective potential relative to the bulk.

In the present article we propose a simple potential-barrier model with a well-defined minimum that reproduces Lang and Kohn's results with a higher degree of accuracy than has been achieved so far by any other potential model.

II. POTENTIAL-BARRIER MODEL

First, we optimize a monotonically increasing potential $V_m(z)$ that approaches the image form far from the surface and saturates the inner potential inside the solid. Then we superimpose on $V_m(z)$ a simple function to reproduce the important minimum in the effective potential found by LK.[8] By this procedure we obtain a simple and nonmonotonic potential $V(z)$. This barrier potential is an improvement with respect to potential-barrier models proposed so far, in which the Friedel oscillations are neglected.

(i) Monotonically increasing potential $V_m(z)$,

$$V_m(z)=\begin{cases} -V_0+V_1\exp(\mu z)\ , & z<0 \\ -W_0\exp(-\nu z)\ , & 0\le z<z_1 \\ -1/[4(z-z_0)]\ , & z\ge z_1\ . \end{cases} \tag{7}$$

The effective potential profile is taken to be of exponential form, and at large distances and well inside the jellium ($z\ll 0$) the potential energy $V_m(z)$ approaches the inner potential V_0. At the jellium edge ($z=0$) it is matched to another exponential function with parameters V_0, V_1, W_0, μ, and ν determined by the constraints that $V_m(z)$ should be continuous and with a continuous derivative at $z=0$. These boundary conditions lead to

$$V_1=V_0-W_0\ , \tag{8}$$

$$\nu=\mu V_1/W_0\ . \tag{9}$$

Therefore V_1 and ν are defined in terms of a set of parameters with a clear physical meaning: V_0, the inner potential of the crystal; W_0, the effective potential at the jellium edge; and μ, the degree of saturation of the barrier.

The remaining parameters z_0 and z_1 are determined by the constraints that $V_m(z)$ should be continuous and with continuous derivative at $z=z_1$;

$$z_1=[\ln(4W_0/\nu)]/\nu\ , \tag{10}$$

$$z_0=z_1-1/\nu\ . \tag{11}$$

Therefore z_0 and z_1 are not independent but are determined in terms of the previously defined set of parameters.

(ii) Nonmonotonically increasing potential $V(z)$,

$$V(z)=V_m(z)-D\,\mathrm{sech}^2[\alpha(z-z_m)]\ , \tag{12}$$

where $\mathrm{sech}(x)=2/[\exp(x)+\exp(-x)]$. This barrier potential model incorporates three parameters (see Fig. 1): z_m, the location of the effective potential minimum (calculated by LK); D, the effective potential minimum depth, relative to the monotonic potential $V_m(z)$; and α,

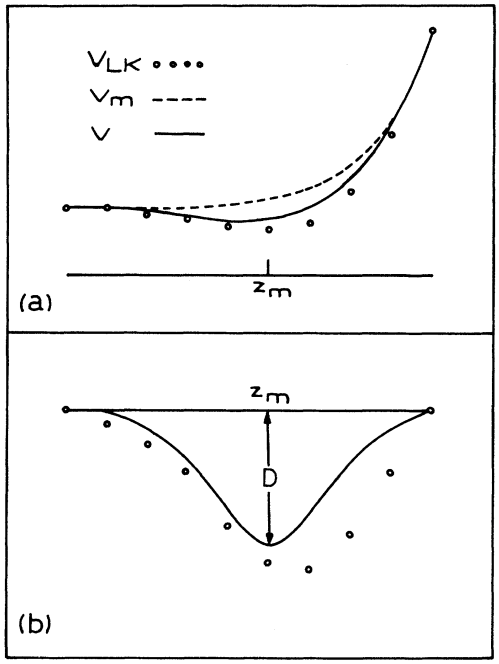

FIG. 1. (a) The effective potential energy of an electron in the vicinity of the jellium surface with $r_s=4$. The open circles are the results calculated by Lang and Kohn, V_{LK} (Ref. 8), and the dashed line represents the monotonic potential V_m of Eq. (7). (b) Difference $V_{LK}-V_m$ (dashed line) and $-D\,\mathrm{sech}^2[\alpha(z-z_m)]$ (solid line).

the width of the effective potential well. Parameters D and α are adjusted assuming that $V(z) \cong V_m(z)$ beyond the jellium edge ($z=0$).

III. RESULTS

In Tables I–III we compare $V_m(z)$ and $V(z)$ [Eqs. (7) and (12)] with the values proposed by JJW, Eq. (6), and those calculated by LK,[8] for three different values of r_s (r_s is the Wigner-Seitz radius). Figures 2–4 show these potentials in the regions inside and near the jellium edge.

The six independent parameters of Eq. (12) can be represented as polynomial functions of r_s,

$$p(r_s)=a_0+a_1(r_s-2)+a_2(r_s-2)^2 + a_3(r_s-2)^3+a_4(r_s-2)^4 . \quad (13)$$

In Table IV we show the polynominal coefficients for the interval $2 \le r_s \le 6$.

To compare the accuracy of Eqs. (6), (7), and (12), we calculated the mean-square difference $\langle \Delta^2 V \rangle$ between the values proposed by the previous approximations $V(z_i)$ and those of LK, V_{LK}, for different r_s values (see Fig. 5):

$$\langle \Delta^2 V \rangle = (1/n) \sum_{i=1}^{n} [V(z_i) - V_{\mathrm{LK}}(z_i)]^2 . \quad (14)$$

TABLE I. Effective potential of (a) Lang and Kohn V_{LK}; (b) JJW, Eq. (6) (Ref. 3) V_{JJW}; (c) monotonic, Eq. (7), V_m; and (d) nonmonotonic, Eq. (12), V (in atomic units) vs the perpendicular coordinate z in atomic units and x in the units chosen by Lang and Kohn, with $r_s=2$.

x	z	V_{LK}	V_{JJW}	V_m	V
−1.00	−6.548	−0.604	−0.605	−0.604	−0.604
−0.95	−6.221	−0.604	−0.605	−0.604	−0.604
−0.90	−5.893	−0.604	−0.605	−0.604	−0.604
−0.85	−5.566	−0.604	−0.605	−0.604	−0.604
−0.80	−5.238	−0.604	−0.605	−0.604	−0.604
−0.75	−4.911	−0.604	−0.605	−0.604	−0.604
−0.70	−4.584	−0.604	−0.604	−0.604	−0.604
−0.65	−4.256	−0.603	−0.604	−0.603	−0.604
−0.60	−3.929	−0.603	−0.604	−0.603	−0.604
−0.55	−3.601	−0.603	−0.603	−0.602	−0.604
−0.50	−3.274	−0.602	−0.602	−0.601	−0.604
−0.45	−2.947	−0.601	−0.600	−0.600	−0.605
−0.40	−2.619	−0.601	−0.598	−0.598	−0.604
−0.35	−2.292	−0.599	−0.594	−0.595	−0.602
−0.30	−1.964	−0.597	−0.588	−0.590	−0.596
−0.25	−1.637	−0.591	−0.579	−0.583	−0.588
−0.20	−1.310	−0.581	−0.567	−0.571	−0.574
−0.15	−0.982	−0.564	−0.548	−0.554	−0.556
−0.10	−0.655	−0.535	−0.522	−0.528	−0.529
−0.05	−0.327	−0.490	−0.487	−0.487	−0.488
0.00	0.000	−0.425	−0.442	−0.425	−0.425
0.05	0.327	−0.357	−0.387	−0.360	−0.360
0.10	0.655	−0.302	−0.325	−0.305	−0.305
0.15	0.982	−0.258	−0.267	−0.258	−0.258
0.20	1.310	−0.222	−0.221	−0.219	−0.219
0.25	1.637	−0.193	−0.186	−0.185	−0.185
0.30	1.964	−0.168	−0.159	−0.157	−0.157
0.35	2.292	−0.148	−0.137	−0.133	−0.133
0.40	2.619	−0.130	−0.119	−0.113	−0.113
0.45	2.947	−0.115	−0.105	−0.099	−0.099
0.50	3.274	−0.102	−0.094	−0.087	−0.087
0.55	3.601	−0.090	−0.084	−0.078	−0.078
0.60	3.929	−0.080	−0.077	−0.071	−0.071
0.65	4.256	−0.071	−0.070	−0.065	−0.065
0.70	4.584	−0.063	−0.064	−0.060	−0.060
0.75	4.911	−0.056	−0.059	−0.056	−0.056
0.80	5.238	−0.050	−0.055	−0.052	−0.052
0.85	5.566	−0.044	−0.052	−0.049	−0.049
0.90	5.893	−0.039	−0.048	−0.046	−0.046
0.95	6.221	−0.035	−0.045	−0.043	−0.043
1.00	6.548	−0.031	−0.042	−0.041	−0.041

The summation in Eq. (14) is extended from $z=-(16/3\pi)^{2/3}r_s/5$ up to the jellium edge $z=0$. The summation starts at that coordinate value because the difference between the effective potential $V_{\mathrm{LK}}(z)$ and the bulk value V_0 is less than 1%. The summation is extended to $z=0$ because, beyond the jellium edge, the values calculated by LK do not approximate the image potential. The n values z_i in the summation are those given by LK,[8] where

$$z_i=2\pi x_i/k_F\ ,\quad i=1,2,\ldots,n\ . \tag{15}$$

z_i is the coordinate in atomic units, k_F is the Fermi wave vector, and x_i is the coordinate chosen by LK.

IV. DISCUSSION AND CONCLUSIONS

From Tables I–III and Figs. 2–4 we learn that the monotonic potential $V_m(z)$, Eq. (7), approaches the classical image form at a large distance from the surface ($z>z_1$) and saturates as the electron approaches the surface and goes over smoothly to a value V_0 determined by electron-electron interactions in the bulk. From Fig. 5 we learn that, except for very low electron densities $r_s\cong 6$, the monotonic potential $V_m(z)$ reproduces LK results with a higher degree of accuracy than that achieved by the JJW barrier model.[3] Because of the simplicity of $V_m(z)$ it would be easier to find analytical solutions of the Schrödinger equation with the potential of Eq. (7) than that of Eq. (6) of JJW.

From Figs. 2–5 we learn that the nonmonotonic poten-

TABLE II. Same as in Table I with $r_s=4$.

x	z	V_{LK}	V_{JJW}	V_m	V
−1.00	−13.096	−0.227	−0.230	−0.228	−0.228
−0.95	−12.441	−0.227	−0.230	−0.228	−0.228
−0.90	−11.786	−0.227	−0.230	−0.228	−0.228
−0.85	−11.131	−0.227	−0.230	−0.228	−0.228
−0.80	−10.477	−0.228	−0.230	−0.228	−0.228
−0.75	−9.892	−0.228	−0.230	−0.228	−0.228
−0.70	−9.167	−0.228	−0.230	−0.228	−0.228
−0.65	−8.512	−0.228	−0.230	−0.228	−0.228
−0.60	−7.857	−0.227	−0.230	−0.228	−0.228
−0.55	−7.203	−0.227	−0.230	−0.228	−0.228
−0.50	−6.548	−0.227	−0.230	−0.228	−0.228
−0.45	−5.893	−0.227	−0.230	−0.227	−0.227
−0.40	−5.238	−0.227	−0.230	−0.227	−0.227
−0.35	−4.585	−0.229	−0.229	−0.227	−0.228
−0.30	−3.929	−0.230	−0.229	−0.227	−0.230
−0.25	−3.274	−0.232	−0.228	−0.226	−0.231
−0.20	−2.619	−0.233	−0.226	−0.225	−0.232
−0.15	−1.964	−0.231	−0.222	−0.222	−0.227
−0.10	−1.310	−0.223	−0.215	−0.216	−0.219
−0.05	−0.655	−0.208	−0.203	−0.204	−0.205
0.00	0.000	−0.181	−0.183	−0.181	−0.181
0.05	0.655	−0.151	−0.155	−0.151	−0.151
0.10	1.310	−0.126	−0.127	−0.126	−0.126
0.15	1.964	−0.106	−0.106	−0.106	−0.106
0.20	2.619	−0.089	−0.090	−0.088	−0.088
0.25	3.274	−0.074	−0.077	−0.074	−0.074
0.30	3.929	−0.061	−0.066	−0.062	−0.062
0.35	4.595	−0.051	−0.058	−0.053	−0.053
0.40	5.238	−0.042	−0.051	−0.047	−0.047
0.45	5.893	−0.034	−0.046	−0.042	−0.042
0.50	6.548	−0.027	−0.041	−0.038	−0.038
0.55	7.203	−0.022	−0.038	−0.034	−0.034
0.60	7.857	−0.017	−0.034	−0.031	−0.031
0.65	8.512	−0.014	−0.032	−0.029	−0.029
0.70	9.167	−0.011	−0.029	−0.027	−0.027
0.75	9.892	−0.009	−0.027	−0.025	−0.025
0.80	10.477	−0.007	−0.025	−0.024	−0.024
0.85	11.131	−0.005	−0.024	−0.022	−0.022
0.90	11.786	−0.004	−0.022	−0.021	−0.021
0.95	12.441	−0.003	−0.021	−0.020	−0.020
1.00	13.096	−0.003	−0.020	−0.019	−0.019

TABLE III. Same as in Table II with $r_s=6$.

x	z	V_{LK}	V_{JJW}	V_m	V
−1.00	−19.644	−0.138	−0.140	−0.139	−0.139
−0.95	−18.661	−0.138	−0.140	−0.139	−0.139
−0.90	−17.679	−0.138	−0.140	−0.139	−0.139
−0.85	−16.697	−0.139	−0.140	−0.139	−0.139
−0.80	−15.715	−0.139	−0.140	−0.139	−0.139
−0.75	−14.733	−0.139	−0.140	−0.139	−0.139
−0.70	−13.751	−0.139	−0.140	−0.139	−0.139
−0.65	−12.768	−0.139	−0.140	−0.139	−0.139
−0.60	−11.786	−0.139	−0.140	−0.139	−0.139
−0.55	−10.804	−0.138	−0.140	−0.139	−0.139
−0.50	−9.822	−0.138	−0.140	−0.139	−0.139
−0.45	−8.840	−0.138	−0.140	−0.139	−0.139
−0.40	−7.857	−0.138	−0.140	−0.139	−0.139
−0.35	−6.875	−0.139	−0.140	−0.139	−0.139
−0.30	−5.893	−0.141	−0.140	−0.139	−0.140
−0.25	−4.911	−0.143	−0.140	−0.138	−0.141
−0.20	−3.929	−0.145	−0.140	−0.138	−0.144
−0.15	−2.947	−0.146	−0.140	−0.138	−0.145
−0.10	−1.964	−0.143	−0.138	−0.136	−0.140
−0.05	−0.982	−0.133	−0.134	−0.131	−0.133
0.00	0.000	−0.116	−0.120	−0.116	−0.116
0.05	0.982	−0.095	−0.097	−0.094	−0.094
0.10	1.964	−0.077	−0.079	−0.076	−0.076
0.15	2.947	−0.062	−0.065	−0.062	−0.062
0.20	3.929	−0.049	−0.055	−0.050	−0.050
0.25	4.911	−0.039	−0.047	−0.043	−0.043
0.30	5.893	−0.030	−0.041	−0.037	−0.037
0.35	6.875	−0.023	−0.036	−0.032	−0.032
0.40	7.857	−0.018	−0.032	−0.028	−0.028
0.45	8.840	−0.013	−0.028	−0.026	−0.026
0.50	9.822	−0.010	−0.026	−0.023	−0.023
0.55	10.804	−0.008	−0.023	−0.021	−0.021
0.60	11.786	−0.006	−0.021	−0.020	−0.020
0.65	12.768	−0.004	−0.020	−0.018	−0.018
0.70	13.751	−0.003	−0.018	−0.017	−0.017
0.75	14.733	−0.002	−0.017	−0.016	−0.016
0.80	15.715	−0.002	−0.016	−0.015	−0.015
0.85	16.697	−0.001	−0.015	−0.014	−0.014
0.90	17.679	−0.001	−0.014	−0.013	−0.013
0.95	18.661	−0.001	−0.014	−0.013	−0.013
1.00	19.644	−0.001	−0.013	−0.012	−0.012

TABLE IV. Polynomial coefficients [Eq. (13)] of the independent parameters V_0, W_0, μ, D, and z_m of Eqs. (7) and (12). The parameter α is given as a function of r_s.

	a_0	a_1	a_2	a_3	a_4
V_0	0.6033	−0.4087	0.1740	−0.0384	0.0033
W_0	0.4247	−0.2564	0.1056	−0.0231	0.0020
μ	1.2300	−0.2823	0.2047	−0.0688	0.0083
D	0.1460	0.3139	−0.2084	0.0756	−0.0081
z_m	−1.1459	−0.5729	0.0000	0.0000	0.0000
α			$0.9118+2.138/r_s$		

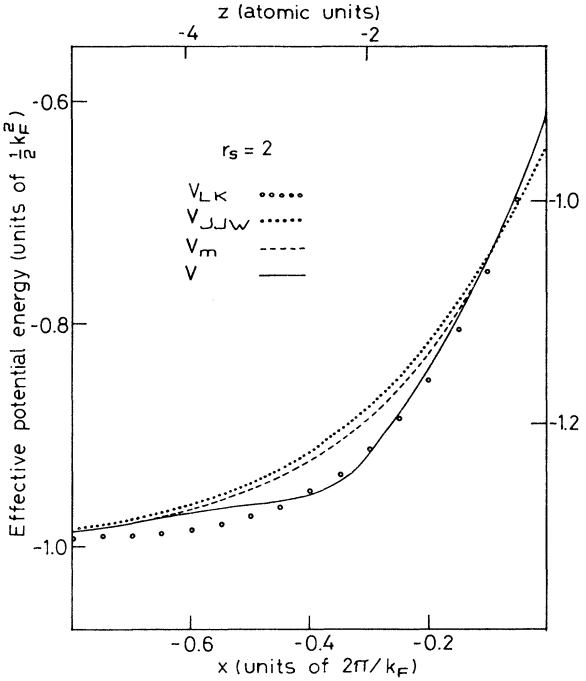

FIG. 2. Comparison of the effective potential energy (in units of $\frac{1}{2}k_F^2$, where k_F is the Fermi wave vector) for an electron in the vicinity of the jellium surface with $r_s=2$. The open circles represent the calculated results of Lang and Kohn (Ref. 8); the dotted curve is the fit obtained using Eq. (6), proposed by JJW (Ref. 3); the dashed line represents the monotonic potential V_m of Eq. (7); and the solid curve is the nonmonotonic potential according to Eq. (12). On the left-hand side the energy zero is at the Fermi level, whereas on the right-hand side it is at the vacuum level.

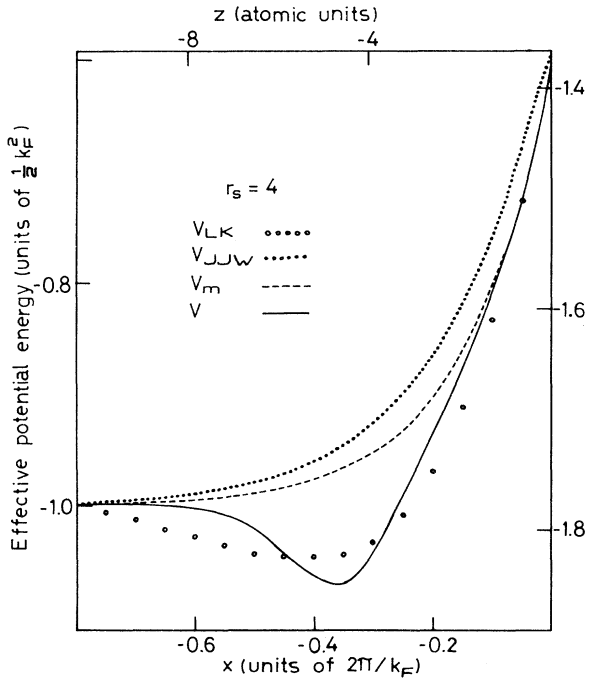

FIG. 3. Same as in Fig. 1 with $r_s=4$.

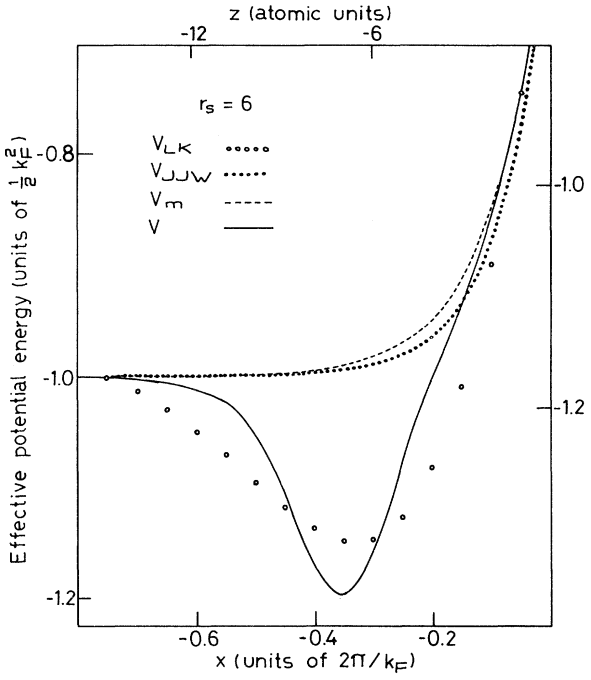

FIG. 4. Same as in Fig. 2 with $r_s=6$.

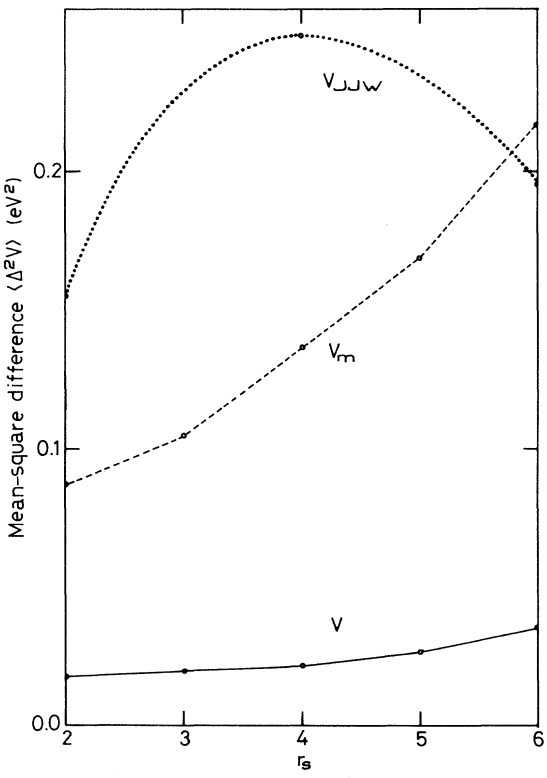

FIG. 5. Mean-square differences $\langle \Delta^2 V \rangle$ between the values calculated by Lang and Kohn and those proposed by (a) JJW, Eq. (6) (dotted line); (b) the present authors (MPV) (dashed line); monotonic potential, Eq. (7); and (c) MPV, nonmonotonic potential, Eq. (12) (continuous line).

tial $V(z)$ introduces an improvement over $V_m(z)$ because it approximates the more intense peak in the effective potential calculated by LK, which is a consequence of Friedel oscillations, especially at low electron densities. To our knowledge, this important characteristic of the potential has not been taken into account by any of the previously proposed barrier models.

The proposed approximation, Eqs. (7) and (12), of the effective potential makes the barrier model suitable for use within more general problems, particularly in tunneling,[10] photoemission, field emission, thermionic emission, inverse photoemission, LEED from crystal surfaces, the interpretation of scanning tunnel microscope experiments,[11] surface work-function changes upon water absorption,[12] and the capacitance of metal-electrolyte interface[13] and thin metal films.[14]

ACKNOWLEDGMENTS

This research project was financially supported by the Consejo Nacional de Investigaciones Cientificas y Tecnicas, Universidad Nacional de La Plata, and the Comisión de Investigaciones Cientificas de la Provincia de Buenos Aires. The authors are also indebted to Fundación Antorchas for a grant and to the Calculus Center of the Universidad Nacional de La Plata (CESPI). We gratefully acknowledge suggestions by J. C. Boettger and a critical reading of the manuscript made by Professor L. Blum.

---

*Author to whom correspondence should be addressed.

[1]S. Thurgate and G. Hitchen, Appl. Surf. Sci. **24**, 202 (1985).
[2]G. Hitchen and S. M. Thurgate, Surf. Sci. **197**, 24 (1988).
[3]P. J. Jennings, R. O. Jones, and M. Weinert, Phys. Rev. B **37**, 6113 (1988).
[4]R. O. Jones and P. J. Jennings, Surf. Sci. Rep. **9**, 165 (1988).
[5]M. N. Read and P. J. Jennings, Surf. Sci. **74**, 54 (1978).
[6]R. E. Dietz, E. G. McRae, and R. L. Campbell, Phys. Rev. Lett. **45**, 1280 (1980).
[7]C. Gaubert, R. Baudoing, Y. Gauthier, J. C. LeBosse, and J. Lopez, J. Phys. C **16**, 2625 (1983).
[8]N. D. Lang and W. Kohn, Phys. Rev. B **1**, 4555 (1970).
[9]E. E. Mola and J. L. Vicente, J. Chem. Phys. **84**, 2876 (1986).
[10]E. E. Mola, C. A. Paola, and J. L. Vicente, *Thin Films and Small Particles,* edited by M. Cardona and J. Giraldo (World Scientific, Singapore, 1989), Vol. 11, p. 105.
[11]J. Wiechers, T. Twomey, D. M. Kolb, and R. J. Behm, J. Electroanal. Chem. **248**, 451 (1988).
[12]E. E. Mola and J. L. Vicente, Surf. Sci. **172**, 533 (1986).
[13]E. E. Mola, R. A. Montani, and J. L. Vicente, J. Electroanal. Chem. **285**, 25 (1990).
[14]J. L. Vicente, C. A. Paola, A. Razzitte, E. E. Mola, and S. B. Trickey, Phys. Status Solidi B **155** K93 (1989).